

XANTHAN GUM AND GUAR GUM – POTENTIAL GREEN INHIBITORS FOR SCALE FORMATION

Andra TĂMAȘ^a, Laura COCHECI^{a*} , Lavinia LUPA^a 

ABSTRACT. Unwanted scale deposits cause numerous technical and economic problems and, for this reason, it is desired to inhibit their formation. The paper studied the possibility of using guar gum and xanthan gum as scale inhibitors mainly in the food industry, due to the fact that they are biodegradable and non-toxic. The two gums, with concentrations between 50 and 100 mg/L, have proven their effectiveness in the case of waters with initial total hardness below 10 mval/L. The scaling inhibition capacity was also correlated with the variation in electrical conductivity of the water samples. X-ray diffraction analysis of CaCO₃ scale formed in waters with initial total hardness over 10 mval/L, stationed for 24 hours in a thermostatic oven at 80°C, demonstrates the presence, mainly, of two polymorphic forms, calcite and aragonite.

Keywords: *calcium carbonate, guar gum, hardness, inhibitor, water scales, xanthan gum*

INTRODUCTION

Hard water is a water that contains a high percentage of calcium and magnesium ions coming from its passage through calcareous layers, mostly made up of calcium and magnesium carbonates, bicarbonates and sulphates.

When hard water is subject to changes in temperature, pressure or velocity, the dissolved minerals precipitate out of the solution and migrate to the area where the fluid has the lowest velocity (usually the inner surfaces of the pipes and equipment), making difficult the fluid flow. Thus, a scale is formed that acts as an insulator.

^a Politehnica University Timișoara, Faculty of Chemical Engineering, Biotechnologies and Environmental Protection, 6 Vasile Pârvan Bd., RO-300223, Timișoara, Romania

* Corresponding author: laura.cocheci@upt.ro



Undesirable scale deposits cause many technical and economical problems: partial or total obstruction of pipes leading to a decrease in flow rate, valves blockage and filters fouling, as well as the decreasing of heat transfer [1]. This last aspect is related to the increase of the thermal resistance to conduction, both in terms of increasing the thickness of the scale layer, as well as due to its low thermal conductivity which gives it insulating properties. The increase of the thermal resistance to conduction has as a consequence the decrease of the overall heat transfer coefficient and, subsequently, the need to increase the surface of heat transfer. Thus, at 2 mm thick deposit, depending on the chemical composition of water scale, the thermal flow is reduced for 10% to 40% [2].

The formation of scales can be done either by deposition (adhesion) of salts on surfaces in contact with aqueous solutions (especially at high temperatures) or by precipitation [3], and results from the succession of two distinct phases: germination and growth [1]. The most important factor that determines the intensity of scale formation is the level of supersaturation of the species that form deposits. Most of the scale-forming salts (CaCO_3 , CaSO_4 , $\text{Mg}(\text{OH})_2$) have inverse solubility characteristics, meaning that their solubility decreases with temperature increasing [3,4]. Scale deposits are mainly composed from calcium carbonate which precipitates in three different forms: calcite, aragonite and vaterite [2].

Scale deposition can be controlled by chemical or physical methods that affect the salts solubility, can prevent the growth of crystals or change the potential of solid surfaces [5]. Scale inhibitors are chemical substances that are added to the solution to stop nucleation, growth and deposition of crystals on a solid surface. Their effectiveness depends on pH, temperature, type of divalent ions and other chemicals compounds in the solution [6].

Traditional scale inhibitors include phosphorus-based compounds, both organic (phosphates, aminophosphates, phosphinocarboxylic acids, phosphonates) and inorganic (polyphosphates). Other classes of compounds that have prove their effectiveness as scale inhibitors are of a polymeric nature – polymers containing phosphate groups, sulfonate groups (polysulfonic acid, polyethylene sulfonic acid), carboxylic acids (polyacrylic, polymethacrylic, polymaleic, polyamino polyether acid methylene phosphonic) [7,8], maleic acid-acrylic acid copolymers, respectively maleic acid – acrylamide with close molecular weights [9]. A particular efficiency in preventing the formation of CaCO_3 scales in seawater desalination processes presents polyacrylic acid with low molecular weight and hydrophobic end groups of medium length (hexyl/cyclohexyl isobutyrate) or long end groups (hexadecyl isobutyrate), such as polyacrylic acid with high molecular weight and hydrophobic end groups with medium length (hexyl isobutyrate) [7].

Phosphorus-based inhibitors are particularly effective in that they can disperse water-insoluble inorganic salts, prevent or interfere with the precipitation and scaling of insoluble inorganic salts on the metal surface and maintain a better heat transfer effect in metal equipment [10]. On the other hand, a large part of them are pollutants for the environment, so it is necessary to replace them with “green” inhibitors, with a high degree of biodegradability. Thus, the following have been successfully used: polyaspartic acid or polyaspartic acids with narrow dispersity and controllable chain length, inulin, carboxymethyl inulin, folic acid polyepoxysuccinic acid [6, 11-14] or its sodium salt [15], polyethyleneimine, polyethyloxazoline, polyaminoamide-type dendrimers [4], depolymerized carboxyalkyl polysaccharide-type biodegradable inhibitors having a degree of substitution of up to 3 carboxylic groups per sugar unit [16], carboxymethylcellulose and its combination with hydroxyethylcellulose [17], fluorescent-tagged scale inhibitor containing fluorescent monomer, acrylic acid and chitosan [18], inhibitor based on Aloe Vera gel [19], extracts from leaves, flowers, fruits, seeds and rhizomes [20-32], pomegranate peel extracts [33], the mixture formed by vitamins B1 and B6 [34].

Recent research also focuses on the use of phosphonates with low phosphorus content, respectively on the implementation of biodegradable fragments in polyacrylate matrices to improve biodegradability [35].

The food industry plays an important role in everyday life, and it is a branch in which the appearance of scales in various technological processes must be avoided all the more. Based on our literature review, we did not find specific studies addressing the use of scale inhibitors for mineral waters utilized in the food industry. Thus, the purpose of this work is to evaluate the efficiency of some non-phosphoric “green” scale inhibitors that can be used successfully in the food industry. Therefore, the effectiveness of guar gum and xanthan gum as scale inhibitors was studied, taking into account that the two gums are used in this industry as stabilizing and thickening agents.

RESULTS AND DISCUSSION

The variation of total hardness for the samples without scale inhibitor, after standing in the oven at 80°C for 24 hours, is shown in Figure 1a (sparkling water) and Figure 1b (still drinking water).

For the same blank samples, the variation in temporary hardness after standing in the oven at 80°C for 24 hours is shown in Figure 2a (sparkling water) and Figure 2b (still drinking water).

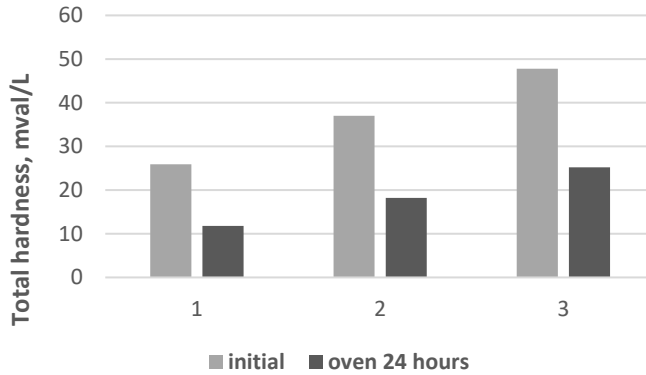


Figure 1a. Variation of total hardness in sparkling water blank samples
1 – $H_t = 25.9$ mval/L; 2 – $H_t = 37$ mval/L; 3- $H_t = 47.8$ mval/L

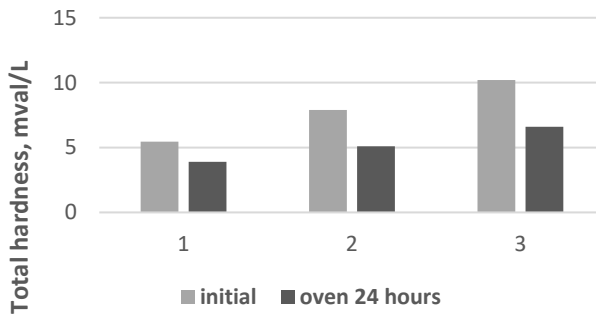


Figure 1b. Variation of total hardness in still drinking water blank samples
1 – $H_t = 5.45$ mval/L; 2 – $H_t = 7.9$ mval/L; 3- $H_t = 10.2$ mval/L

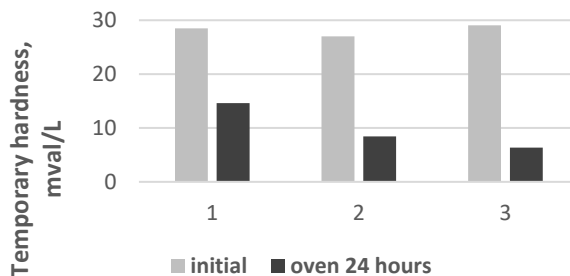


Figure 2a. Variation of temporary hardness in sparkling water blank samples
1 – $H_t = 25.9$ mval/L; 2 – $H_t = 37$ mval/L; 3- $H_t = 47.8$ mval/L

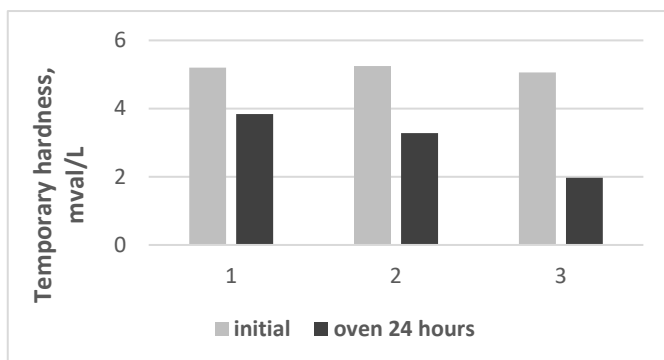


Figure 2b. Variation of temporary hardness in still water blank samples
1 – $H_t = 5.45$ mval/L; **2** – $H_t = 7.9$ mval/L; **3**– $H_t = 10.2$ mval/L

It is found that both the total and the temporary hardness of the sparkling water are clearly higher to those of still drinking water, both before and after standing in the oven. Also, the initial temporary hardnesses for each type of water are approximately equal, regardless of the initial value of total hardness. The percentages of decrease in total and temporary hardness, after keeping the samples in the oven, are shown in Figure 3.

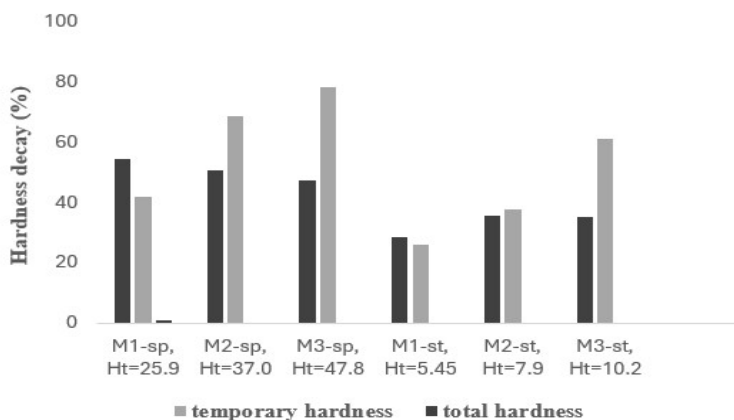


Figure 3. Decrease in temporary/total hardness of the blank samples after standing in the oven

It is observed that the hardness decay slow down with the increasing of total hardness within sparkling water. On the other hand, the increasing of temporary hardness facilitates the hardness decay for both type of studied waters.

For sparkling and still water samples treated with xanthan gum (XG) or guar gum (GG) (concentration 50mg/L or, respectively, 100mg/L) and kept in the oven under identical conditions to the blank samples, the efficiency of the scale inhibitor, calculated with rel. (1), is shown in Figures 4a and 4b.

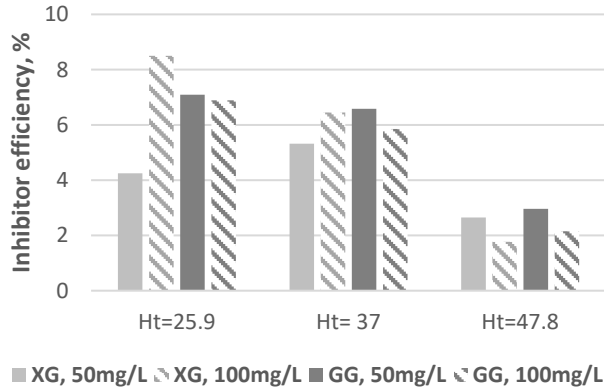


Figure 4a. The efficacy of xanthan/guar gums as scale inhibitor for sparkling water

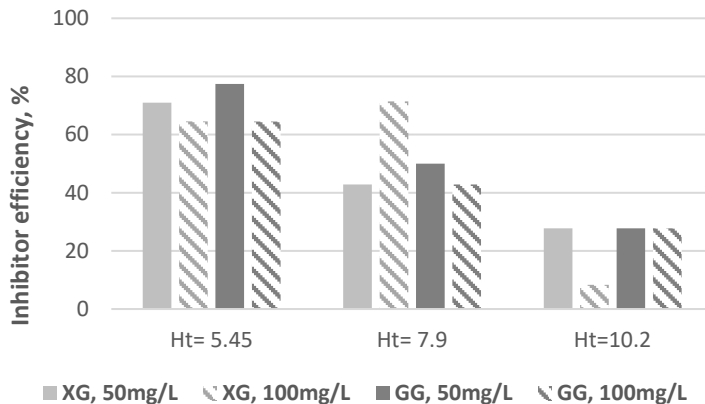


Figure 4b. The efficacy of xanthan/guar gums as scale inhibitor for still water

The two gums are found to be most effective in waters with lower initial hardness. Also, doubling the xanthan/guar gum concentration does not significantly influence the scale inhibition efficiency.

The effectiveness of xanthan/guar gum as scale inhibitor in waters with different total hardnesses was also verified by measuring electrical conductivity (σ), before and after standing in the oven, Table 1.

Table 1. Variation of electrical conductivity of water samples in the presence of scale inhibitors

Initial values	<i>Inhibition efficiency (%) / Electrical conductivity, $\mu\text{S/cm}$</i>				
	blank	XG 50mg/L	XG 100mg/L	GG 50mg/L	GG 100mg/L
$H_{\text{tot},i} = 5.45$ mval/L $\sigma_i = 490$ $\mu\text{S/cm}$	0 / 390	70 / 470	65 / 460	78 / 480	63 / 380
$H_{\text{tot},i} = 7.9$ mval/L $\sigma_i = 810$ $\mu\text{S/cm}$	0 / 541	42.9 / 676	71.4 / 794	50 / 755	42.9 / 686
$H_{\text{tot},i} = 25.9$ mval/L $\sigma_i = 1900$ $\mu\text{S/cm}$	0 / 1326	4.25 / 1361	8.5 / 1398	7.1 / 1389	-

The lower values of the efficiency of inhibiting the formation of scales in the case of the two gums are correlated with a more pronounced decrease in electrical conductivity, as a consequence of the reduction of ions number in the solution, therefore of the formation of scales.

The mechanism of crystal growth inhibition by the two gums can be explained by the electrostatic interaction between the partially negative charge of the functional groups of the inhibitor (OH groups or ether oxygen atoms) and the positive charges of the ions in the solution, according to [36]. The monosaccharide residues in the two gums contain multiple polar, hydroxylic groups which, through the density of electrons (non-participating p) constitute centers that electrostatically attract cations. Also, in the case of xanthan gum, a chemical adsorption between the carboxyl groups of glucuronic acid (C1:C6) and the cations in the solution is also possible.

In the case of water samples in which the efficiency of xanthan/guar gums had low values, the X-ray diffraction analysis of the precipitates formed after standing in the oven was carried out. Thus, for the blank sample of sparkling water having the initial total hardness of 25.9 mval/L, the X-ray diffractogram is presented in Figure 5a. For the water samples with the same initial hardness but with the addition of xanthan/guar gum (concentration 50mg/L), the corresponding diffractograms are shown in Figures 5b and 5c.

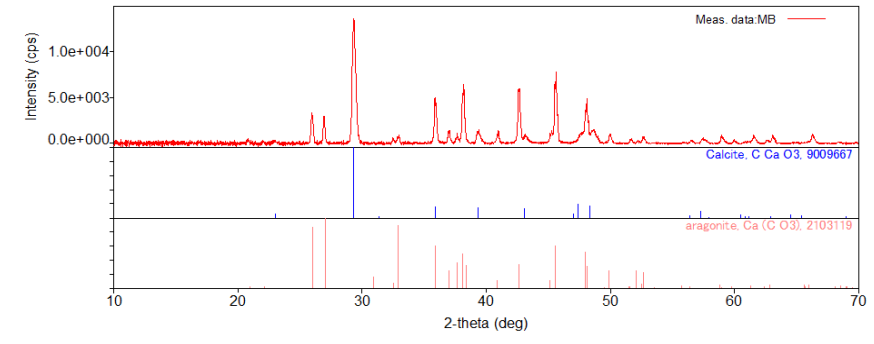


Figure 5a. X-ray diffractogram of CaCO_3 formed from the water sample with initial total hardness 25.9 mval/L

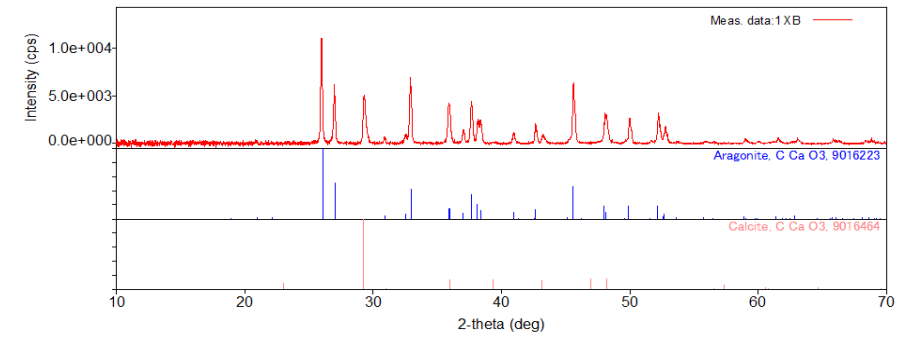


Figure 5b. X-ray diffractogram of CaCO_3 formed from the water sample with initial total hardness 25.9 mval/L and addition of XG 50mg/L

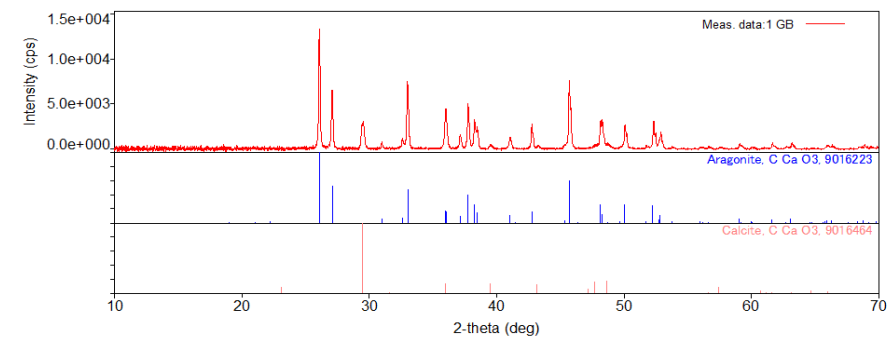


Figure 5c. X-ray diffractogram of CaCO_3 formed from the water sample with initial total hardness 25.9 mval/L and addition of GG 50mg/L

From the analysis of the three diffractograms it can be seen that the precipitate, formed after standing in the oven of the water sample without gums (sample MB in Figure 5a), has calcite (COD file 9009667) as its main phase and aragonite (COD file 2103119) as secondary phases. This fact is in accordance with a study regarding the characterization of powders obtained by drying natural sparkling mineral waters from public springs in Borsec which reveals that the dominant mineral (over 50% wt) is calcite [37]. Also, the precipitates formed after standing in the oven of the water samples with 50mg/L xanthan gum (sample 1XB in Figure 5b) and with 50mg/L guar gum (sample 1GB in Figure 5c) have aragonite (COD file 9016223) as the main phase, and as secondary phase calcite (COD file 9016464). It is observed that the intensity of the main peak in the diffractogram of the MB material, located at $2\theta = 29.3^\circ$ and corresponding to the calcite, is lower in the diffractograms of the 1XB and 1GB materials. At the same time, the first two peaks, located at 2θ of 26.0° and 27.0° and attributed to aragonite, have the most pronounced intensities in the 1XB and 1GB diffractograms compared to the MB diffractogram.

X-ray diffraction analysis of the precipitates demonstrates that, generally, the gums favor the crystallization of calcium carbonate in the form of aragonite as the main phase. The statement is also supported by data from the literature [38] which concludes that the main crystalline phase of CaCO_3 changes from calcite to aragonite after the addition of scale inhibitors.

CONCLUSIONS

Water samples with different values of the initial total hardness (natural or obtained by adding CaCl_2), to which aqueous solutions of guar gum or xanthan gum were added so that their concentration in the final solution was between 50mg/L and 100mg/L, were subjected to analysis. Xanthan gum and guar gum are part of the carbohydrate class, being natural, non-toxic and accessible polysaccharides that can be modified into more advantageous forms.

Both types of gums have proven their effectiveness in the inhibiting the formation of scales in waters with initial total hardness lower than 10mval/L.

Taking into account that low hardness waters are used in the processes of the food industry, the use of these types of gums as scale inhibitors has many benefits compared to the toxic inorganic inhibitors used regularly: (1) compatibility with the environment due to the fact that they are natural, biodegradable compounds; (2) high inhibition efficiency; (3) low costs

due to the fact that these gums are found in food industrial processes as stabilizing and thickening agents, thus minimizing the addition of additional reagents.

EXPERIMENTAL SECTION

Samples preparation and the working method

The analyzes were performed on still drinking water or sparkling water (products of the same company) without or with the additional addition of calcium salt (CaCl_2) to obtain a predetermined value of total hardness. The composition of the samples used in this study is presented in Table 2. From each type of water, 250 mL were measured to which were added the corresponding amounts of guar gum or xanthan gum aqueous solutions (initial concentrations of 1g/L and, respectively 2g/L), so that their final concentrations were either 50mg/L or 100mg/L. The flasks with water, covered, were placed in the thermostatic oven at 80°C for 24 hours. At the end of the stationary time in the oven, the water samples were cooled, filtered and were determined by titration their total and temporary hardness. These types of hardness were also measured before placing the samples in the oven. Both guar gum and xanthan gum were purchased from Sigma-Aldrich.

The electrical conductivity of the water samples, before and after the stationary time in the oven, was measured with a Multi 3320 WTW conductometer.

The phase composition of some of the precipitates collected on the filter paper was made using a Rigaku Ultima IV diffractometer (40 kV, 40 mA), equipped with a D/teX Ultra detector, using $\text{Cu}_{K\alpha}$ ($\lambda = 0,15406$ nm) radiation, in range $2\theta = 10-70^\circ$, with speed of 5°/min and step of 0.01°. The assignment of the peaks corresponding to the crystalline phases present in the samples was performed by the Rigaku diffractometer software using the COD database [39].

Determination of the total and temporary hardness and calculation of scale inhibition effectiveness

The temporary hardness was determined by titrating a known volume of hard water with a 0.1N hydrochloric acid solution with a known factor, in the presence of methyl orange as indicator according to [40]. The total hardness was determined by the complexometric method, which involves titrating the sample with a solution of complexon III 0.01M (disodium salt of ethylenediaminetetraacetic acid – EDTA disodium salt) in the presence of Eriochrome Black T as indicator, at a pH value between 9 and 10, according to [40].

The scale inhibition efficiency (E) was calculated with rel. (1):

$$E = \frac{d_2 - d_1}{d_0 - d_1} \cdot 100 \quad (1)$$

where: d_0 - initial total hardness, d_1 – the total hardness of the blank sample after the oven, d_2 – the total hardness of the sample with inhibitor after the oven.

Table 2. Water samples composition

Sample	CaCl ₂ added (g/L)	Total hardness (mval/L)	Temporary hardness (mval/L)
M1-st	-	5.45	5.20
M2-st	0.1360	7.90	5.60
M3-st	0.2829	10.2	5.06
M1-sp	-	25.9	28.5
M2-sp	0.6160	37.0	28.8
M3-sp	1.3407	47.8	29.1

REFERENCES

1. D. Liu; *Research on performance evaluation and anti-scaling mechanism of green scale inhibitors by static and dynamic methods*, PhD Thesis, L'Ecole Nationale Supérieure d'Arts et Métiers Paris Tech, France, **2011**, pp.12-14
2. D. Dobersek; D. Goricanec; *Int. J. Math. Models Methods Appl. Sci.*, **2007**, 1(2), 55-61
3. Z. Amjad; P.G. Koutsoukos; *Desalination*, **2014**, 335, 55-63
4. D. Hasson; H. Shemer; A. Sher; *Ind. & Eng. Chem. Res.*, **2011**, 50, 7601-7607
5. J. MacAdam; S.A. Parsons; *Rev. Environ. Sci. Biotechnol.*, **2004**, 3, 159-169
6. R. Erany; *A study of scale and scaling potential during high salinity and low salinity waterflooding*, Master's Thesis, University of Stavanger, Norway, **2016**, pp. 23-32
7. A.A. Al-Hamzah; C.M. Fellows; *Desalination*, **2015**, 359, 22-25
8. C.B. Chew; R. Mat; *Chem. Eng. Trans.*, **2015**, 45, 1471-1476
9. B. Senthilmurugan; B. Ghosh; S.S. Kundu; M. Haroun; B. Kameswari; *J. Pet. Sci. Eng.*, **2010**, 75 (1-2), 189-195
10. W. Wand; Y-G. Yi; Z-F. Sun; S-B. Dong; W-C. Du; *Key Eng. Mater.*, **2019**, 814, 511-516
11. D. Liu; W. Dong; F. Li; F. Hui; J. Ledion; *Desalination*, **2012**, 304, 1-10
12. D. Peronno; H. Cheap-Charpentier; O. Horner; H. Perrot; *J. Water Process Eng.*, **2015**, 7, 11-20
13. M-L. Zhang; Z. Ruan; Y. Han; Z-W. Cao; L. Zhao; Y-Q. Xu; Z-Y. Cao; W-Y. Shi; Y. Xu; *Desalination*, **2024**, 570, 117080
14. A. Mohseni; L. Mahmoodi; M.R. Malayeri; *Adv. Powder Technol.*, **2023**, 34, 103954
15. X. Zhou; Y. Sun; Y. Wang; *J. Environ. Sci.*, **2011**, 23, S159-S161
16. F. De Campo; S. Kesavan; G. Woodward; *Polysaccharide based scale inhibitor*, European Patent EP 2 148 908 B1, **2010**

17. R.S. Fernandes; W.D.L. Santos; D.F. de Lima; M.A.F. de Souza; B.B. Castro; R.C. Balaban; *Desalination*, **2021**, 515, 115201
18. S. Zhang; J. Ding; D. Tian; M. Chang; X. Zhao; M. Lu; *J. Mol. Struct.*, **2023**, 1272, 134157
19. L. Castillo; E. Torin; J.A. Garcia; M. Carrasquero; M. Novas; A. Vilorio; *New product for inhibition of calcium carbonate scale in natural gas and oil facilities based on Aloe Vera: Application in venezuelan oilfields*, Latin American and Caribbean Petroleum Engineering Conference, Cartagena, **2009**, SPE-1230077-PP
20. M.A.J. Mazumder; *Coatings*, **2020**, 10, 928-956
21. Z. Belarbi; J. Gamby; L. Makhloufi; B. Sotta; B. Tribollet; *J. Cryst. Growth*, **2014**, 386, 208-214
22. Z. Belarbi; B. Sotta; L. Makhloufi; B. Tribollet; J. Gamby; *Electrochim. Acta*, **2016**, 189, 118-127
23. O. Horner; H. Cheap-Charpentier; X. Cachet; H. Perrot; J. Ledion; D. Gelus; N. Pecoul; M. Litaudon; F. Roussi; *Desalination*, **2017**, 409, 157-162
24. A.M. Abdel-Gaber; B.A. Abd-El-Nabey; E. Khamis; D.E. Abd-El-Khalek; *Desalination*, **2008**, 230 (1-3), 314-328
25. A.M. Abdel-Gaber; B.A. Abd-El-Nabey; E. Khamis; D.E. Abd-El-Khalek; *Desalination*, **2011**, 278 (1-3), 337-342
26. Z. Mohammadi; M. Rahsepar; *Res. Chem. Intermed.*, **2018**, 44(3), 2139-2155
27. M. El Housse, A. Hadfi, N. Iberache, I. Karmal, F. El-Ghazouani, S. Ben-Aazza, M. Belattar, I. Ammayen, M. Nassiri, S. Darbal, Y. Riadi, M. Ikiss, A. Driouiche; *Ind. Crops Prod.*, **2024**, 222, 120030
28. Karmal, M. El Housse, A. Hadfi, J. El Gaayda, A. Oulmekki, J.E. Hazm, S. Ben_Aazza, M. Belattar, S. Mohareb, N. Hafid, R.A. Akbour, M. Hamdani, A. Driouiche; *Desalin. Water Treat.*, **2021**, 240, 115-123
29. M. Nassiri, I. Karmal, S. Darbal, M. El Housse, S. Ben-Aazza, M. Belattar, A. Driouiche; *J. Water Process Eng.*, **2024**, 65, 105846
30. E.S. Suharso, A.K. Agung, H.S. Buhani, *Desalin. Water Treat.*, **2019**, 169, 29-37
31. G. Vasyliiev, V. Vorobyova, T. Zhuk, O. Kalinchuk; *Mater. Today Proc.*, **2022**, 50, 477-482
32. Z. Mohammadi; M. Rahsepar; *J. Alloys Compd.*, **2019**, 770, 669-678
33. A.M. Abdel-Gaber; B.A. Abd-El-Nabey; E. Khamis; H. Abd-El-Rhmann; H. Aglan; A. Ludwick; *Int. J. Electrochem. Sci.*, **2012**, 7, 11930-11940
34. R. Menzri; S. Ghizellaoui; M. Tlili; *Desalination*, **2017**, 404, 147-154
35. K.I. Popov; N.E. Kovaleva; G.Y. Rudakova; S.P. Kombarova; V.E. Larchenko; *Therm. Eng.*, **2016**, 63, 122-129
36. A.E. Elkholy; H.F. El-Taib; A.M. Rashad; K.Zakaria; *J.Pet.Sci.Eng.*, **2018**, 166, 263-273
37. S.A. Avram; D.V. Platon; L.B.Tudoran; G.Borodi; I.Petean; *Appl.Sci.-Basel*, **2024**, 14(23), 10806
38. X. Li; B. Gao; Q. Yue; D. Ma et al.; *J. Environ. Sci.*, **2015**, 29, 124-130
39. Crystallography Open Database, <http://www.crystallography.net/cod/>
40. L. Andronic; A. Duță; *Analize fizico-chimice și metode avansate de epurare a apelor uzate*, Ed. Universității Transilvania, Brașov, **2013**.